FLOW FIELD ANALYSIS OF TRUCKS AND A DESIGN OF AN ADDITIONAL DRAG REDUCTION DEVICE

Jianmin Xu[*] - Shuiting Zhou

[1]School of Mechanical and Automotive Engineering, Xiamen University of Technology, Xiamen, Fujian province, China.

ARTICLE INFO

***Article history*:**
Received: 30.11.15.
Received in revised form: 12.03.16.
Accepted: 16.03.16.

Keywords:
Truck
Aerodynamic characteristics
Drag reduction devices
Flow field

Abstract:

Numerical simulation of the outflow field of a truck is carried out by using aerodynamic analysis software based on a computational fluid dynamics model. The velocity and pressure distribution of the outflow field around the truck are obtained and the cause of generating aerodynamic drag is analyzed. The flow separation in the front and at the tail of the truck is the main cause of air resistance generation. Three kinds of truck fairing are proposed based on the aerodynamic drag reduction mechanism. The influence of a drag reduction device on aerodynamic characteristics is analyzed based on the pressure distribution, velocity distribution and turbulent kinetic energy distribution around the truck. The research shows that three kinds of drag reduction devices for a truck have great effect on drag reduction, with the bottom fairing showing the best drag reduction effect. This study provides a theoretical basis for drag reduction and energy saving for the truck.

1 Introduction

With the rapid rise of oil prices, there is a growing emphasis on drag reduction and other forms of energy-saving designs in the automotive industry. Air resistance of vehicles is proportional to the square of the vehicle speed. When vehicle speed gradually increases, the proportion of aerodynamic drag also increases. Fuel efficiency generated by reducing the aerodynamic drag will be considerable. Due to the unique structure of the truck, the aerodynamic shape is poor. It has a large frontal area so that the aerodynamic drag is large. At high speeds, the aerodynamic drag of a truck increases rapidly, and the fuel consumption increases sharply. Numerical simulation of a container semitrailer truck was conducted by using CFD software, and significant conclusions were obtained [1-2]. A numerical simulation of the influence of a guide cowl on the aerodynamic characteristics of a light-duty van was researched [3]. A 3D numerical simulation on the exterior flow field of a round roof van was conducted based on a model set up. Four types of spoilers were designed and simulated to optimize the aerodynamic performance of the van [4]. The aerodynamic balance force and time-averaged wall pressure distribution measurements were conducted in a wind tunnel to investigate the aft-body drag reduction of the tractor-trailer truck model by all add-on devices [5]. The bottom separator installation can improve the aerodynamic characteristics of light vans and reduce aerodynamic

[*] Corresponding author. Tel.: +13459263068
E-mail address: xujianmin1020@163.com

drag [6]. A passive drag reduction technology for trucks is proposed in [7]. Wang et al. [8] researched the drag reduction mechanism of a truck shroud by using numerical simulation. The effect of the gap between driver cab and freight body of a heavy-duty truck on its aerodynamic characteristics is researched [9]. CFD simulation and wind tunnel tests were performed on a kind of commercial truck to study the influence of the cab shape and various kinds of guide cowls on aerodynamic drag [10]. To measure the aerodynamic drag produced by the vehicle, a wind tunnel study was undertaken using a 1/10 th scale model truck [11]. Three-dimensional flow structures around simplified model vehicles and heavy vehicles were introduced and the flow-control devices used for drag reduction were discussed [12-13]. In order to reduce the aerodynamic drag of a heavy-duty truck, four different shapes and styles of deflectors based on the original one were introduced. The three-dimensional flow structures around simplified model vehicles were introduced and the flow-control devices used for drag reduction were discussed [14]. Simple potential improvements in the aerodynamic design of the light bars were investigated by combining computational fluid dynamics (CFD) with the design of experiments and meta-modeling methods [15]. Simple devices added to the trailer were studied [16], showing that it is possible to decrease the aerodynamic drag by over 10 %, with an increase of overall dimensions below 1 % without any change to the load capacity of the trailer. An experimental investigation of several drag reduction devices installed in the rear of a bluff body with square back geometry in ground proximity was conducted [17].

With the rapid development of highways, the traveling speed of vans and trucks is rising, so studying the aerodynamic characteristics of such vehicles is necessary. In this paper, the outflow field of a van is analyzed in detail by using three-dimensional software and fluid analysis software. Three kinds of van fairing will be proposed based on the analysis, and the optimized drag reduction device is obtained based on the aerodynamic characteristics of the van. This study will provide the theoretical basis for the drag reduction and energy conservation of trucks.

2 Establishment of finite element model of the van

2.1 The establishment of geometric model of the van

The geometric model of the van established by using software UG is shown in Fig. 1. The van model is divided into two parts, which are the cab and the container. Its external scale includes mirrors, door handles, exhaust system and other components which are simplified when establishing the model of the van in order to save computing resources.

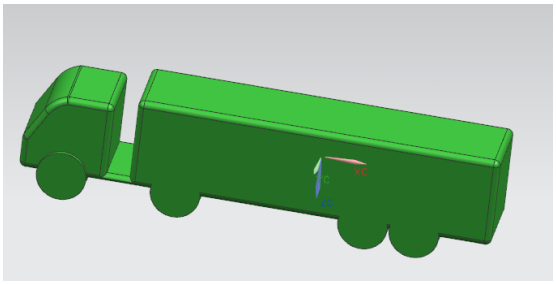

Figure 1. Geometric model of the van.

2.2 Meshing of computational domain

The three dimensional model of the van is imported into Gambit software in the format of parasolid to mesh the computational domain. The cuboid which includes five times the vehicle length, four times the vehicle width and three times the vehicle height is taken as the fluid simulation area. An unstructured grid is used in the computational domain. To improve the calculation accuracy, local mesh refinements are conducted in the surrounding area of the truck. Fig. 2 shows the mesh of computational domain.

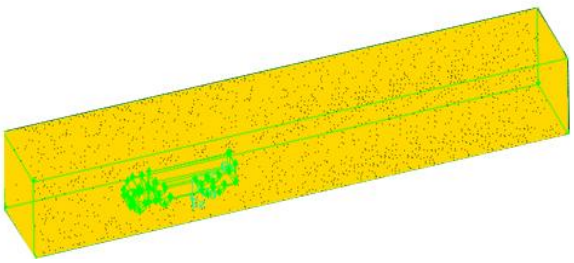

Figure 2. Mesh of computational domain.

2.3 Boundary conditions

(1) Entrance conditions: The end face of the flow direction is taken as the entrance boundary. The coordinate system is built on the van body, with the airflow direction being opposite to the traveling direction of van. The van speed is set to 40 m/s, which is along the x axis direction. The remaining two vectors that are perpendicular to airflow direction are set to 0 m/s. Turbulence intensity is set to 0.5 %.
(2) Export boundary: The distal end surface of the van body is set to the pressure outlet boundary. The relative pressure is set at 0.
(3) Wall boundary conditions: The vertical and horizontal surfaces of the computational domain and the outer surface of the model are all set at a fixed wall boundary condition.

3 Mathematical model

3.1 Control equations

The total mass conservation equation for the compressible flow is as follows:

$$\frac{\partial \rho}{\partial t}+\frac{\partial}{\partial x_i}(\rho u_i)=S_m, \tag{1}$$

where, ρ is the density; t is the time; u_i is the speed tensor; x_i is coordinates tensor.

In the inertial coordinate system, the momentum conservation equation in the direction of i is as follows [18]:

$$\frac{\partial}{\partial t}(\rho u_i)+\frac{\partial}{\partial x_j}(\rho u_i u_j)=-\frac{\partial p}{\partial x_i}+\frac{\partial \tau_{ij}}{\partial_j}+\rho g_i+F_i, \tag{2}$$

where, ρ is the density; t is the time; u_i and u_j are the velocity tensor; x_i and x_j are coordinate tensor; ρg_i is gravity body force; p is static pressure; τ_{ij} is referred to as subgrid scale stress (SGS) which reflects the influence of small-scale vortex motion on solving the equations of motion; F_i is the gravity body force and the other volume force.

3.2 Turbulence Model

The standard κ-ε model is used to calculate the Reynolds stress to close the flow control equation, according to the following equation[19]:

$$\begin{aligned}&-\overline{\rho u_i' u_j'}=\\&-2\mu_t s_{ij}+\frac{2}{3}(\mu_t\frac{\partial u_k}{\partial x_k}+\rho k)\delta_{ij}\end{aligned}, \tag{3}$$

where, μ_t is the turbulent viscosity coefficient, determined by the following equation.

$$\mu_t=\frac{c_\mu \rho \kappa^2}{\varepsilon}, \tag{4}$$

where, k and ε are turbulent kinetic energy and turbulent energy dissipation rate, whose transport equations are as follows.

$$\begin{aligned}&\frac{\partial}{\partial x_j}\left(\rho\mu_j\kappa-\frac{\mu_{eff}}{\sigma_\kappa}\frac{\partial \kappa}{\partial x_j}\right)=\\&\mu_t s_{ij}\frac{\partial u_i}{\partial x_j}-\rho\varepsilon-\frac{2}{3}\left(\mu_t\frac{\partial u_i}{\partial x_i}+\rho\kappa\right)\frac{\partial u_i}{\partial x_i}\end{aligned}, \tag{5}$$

$$\begin{aligned}&\frac{\partial}{\partial x_j}\left(\rho\mu_j\varepsilon-\frac{\mu_{eff}}{\sigma_\varepsilon}\frac{\partial \varepsilon}{\partial x_j}\right)\\&=c_{\varepsilon 1}\frac{\varepsilon}{\kappa}\left\{\mu_t s_{ij}\frac{\partial u_i}{\partial x_j}-\frac{2}{3}\left(\mu_t\frac{\partial u_i}{\partial x_i}+\rho\kappa\right)\frac{\partial u_i}{\partial x_i}\right\},\\&-c_{\varepsilon 2}\rho\frac{\varepsilon^2}{\kappa}+c_{\varepsilon 4}\rho\varepsilon\frac{\partial u_i}{\partial x_i}\end{aligned} \tag{6}$$

where, $\mu_{eff}=\mu+\mu_t$, the empirical coefficients of C_μ, σ_k, σ_ε, $C_{\varepsilon 1}$, $C_{\varepsilon 2}$ and $C_{\varepsilon 4}$ are determined according to Table 1.

Table 1. Experience coefficient [20]

C_μ	σ_k	σ_ε	$C_{\varepsilon 1}$	$C_{\varepsilon 2}$	$C_{\varepsilon 4}$
0.09	1.0	1.22	1.44	1.92	-0.33

The finite volume method is used to disperse the control equation, and the SIMPLE algorithm is used to conduct the numerical simulation.

4 Outflow field analysis of the original model of the van

4.1 Pressure distribution

Fig. 3 shows the pressure contour of the symmetry plane of the van. It can be seen from Fig. 3 that the pressure in front of the van is very high. Positive pressure areas are mainly concentrated in the front of the front windshield, which is the main source of aerodynamic drag. There is a high pressure area in the front region of the cargo compartment, showing that the cargo compartment creates high resistance. It can also be seen in Fig. 3 that the pressure of the front van is greater than that of the rear van, and the pressure drag is created. The pressure at the top of the van is smaller than that of the van bottom, which causes pneumatic lift.

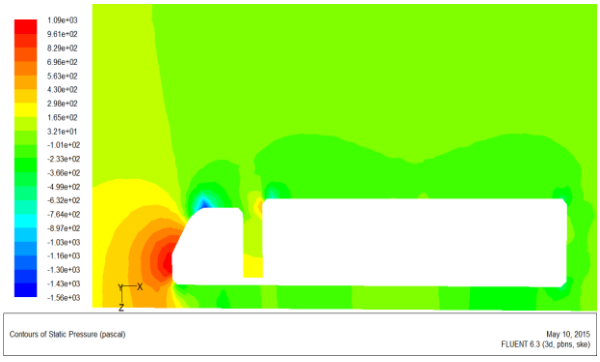

Figure 3. Pressure contour of the symmetry plane of van.

4.2 Velocity distribution

Fig. 4 shows the velocity vector of the symmetry plane of the van. In the block of the van the air flow is divided into two parts. A portion of the airflow flows over the van roof, while the other portion flows below the van bottom. Since the cargo compartment is higher than the cab, the protruding parts block the airflow. Airflow separation is produced at the top of the cab and large vortices are formed. When the stream flows around the van body, the air flow velocity of each portion is not the same, which forms a vortex. Vortices appear around the tail region of van and the area between the van body and the front. The vortex in the rear area of the van is the largest. Because the rear pressure of the van is smaller than the surrounding pressure, a strong vortex area is formed, as shown in Fig. 5.

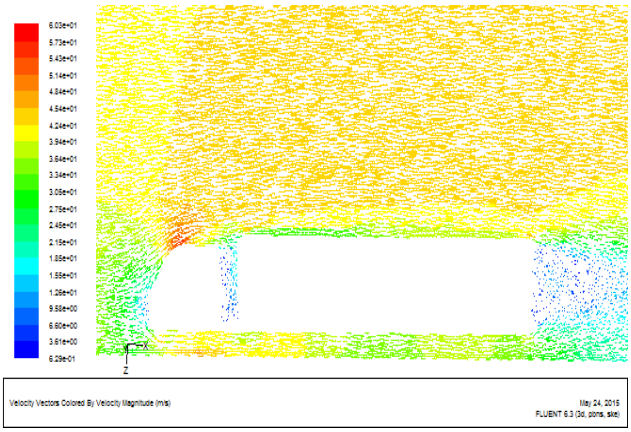

Figure 4. Velocity vector of the symmetry plane of the van.

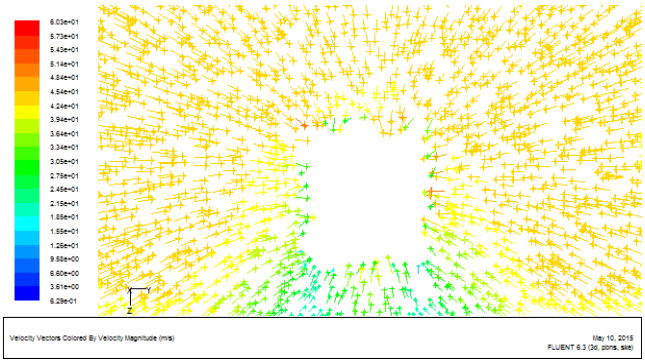

Figure 5. Velocity vector of van tail.

4.3 Turbulent kinetic energy distribution

Turbulent kinetic energy can reflect the size of the turbulent energy losses and the intensity of the turbulence. Fig. 6 shows the contours of turbulent kinetic energy, showing that the turbulent kinetic energy losses are mainly concentrated at the top of the van cab and the rear of the van. This is because the airflow at the top of the cab is obstructed by the cargo compartment and complex vortices are formed. Air stream from the top, side and bottom of the van can produce vortices in the van tail. Affected by the separation of the airflow, the turbulent kinetic energy of the van tail is very large. The turbulent kinetic energy should be avoided as far as possible in order to reduce air resistance of the van.

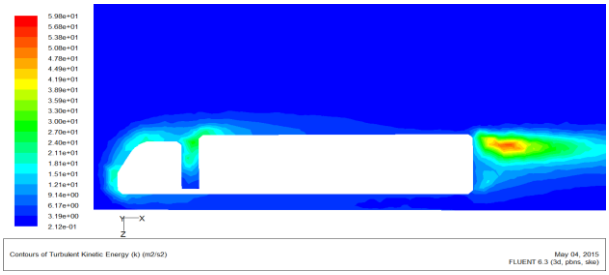

Figure 6. Contour of turbulent kinetic energy.

5 Design and flow field analysis of additional drag reduction device

5.1 Design of drag reduction device in tail and comparative analysis

Based on the computational fluid dynamics analysis of the van, aerodynamic devices are installed at the tail, bottom and front of the van respectively to reduce resistance and fuel consumption. Fig. 7 shows the van model with the drag reduction device at the tail and has a spoiler at the rear of the van's carriage. The baffle can be installed at the top and side edges of the trailing edge of the van. Airflow around the van will flow toward the tail of van with this baffle. Negative pressure behind the vehicle is avoided and air resistance is also reduced. In the end, the fuel consumption of the van is reduced and the travel efficiency is increased.

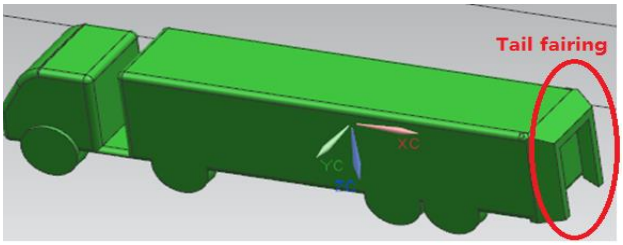

Figure 7. Van model with drag reduction device at the tail.

Since the air pressure of the rear of the van is lower than that of the top and sides of the van, vortices are formed. Fig. 8 presents the contrast of the speed contour of the tail of the van, showing that the low flow region of the van model with the drag reduction device on the tail is significantly reduced. The uniform flow rate of each region can avoid eddy currents caused by the local flow velocity which is very small, and thus the drag forces generated by the eddy currents are reduced. Fig. 9 shows the contrast of the velocity vector of the van tail (Center section). After installing additional rear fairing， due to the diversion effect of transom, the air flow becomes a little more smooth. Because of the regular flow of air, vortex and the van aerodynamic drag are reduced.

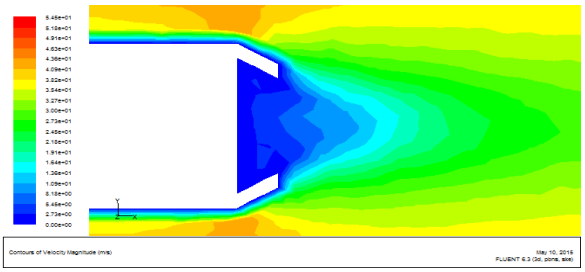

a) Van model with drag reduction device on the tail

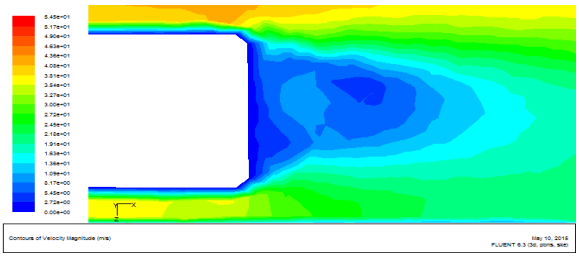

b) Original model

Figure 8. The contrast of speed contour of the van tail (top view).

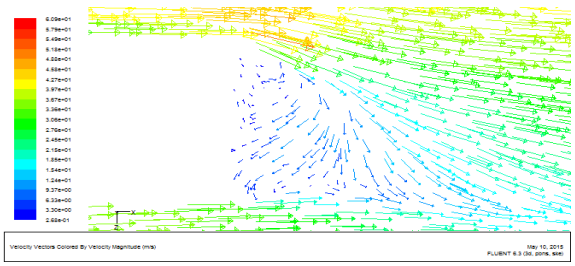

a) The van model with drag reduction device in tail

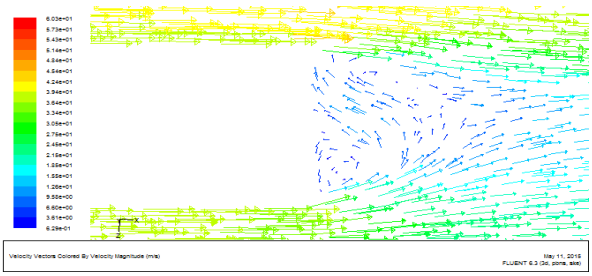

b) The original model

Figure 9. The contrast of the velocity vector of van tail (Center section).

Fig. 10 presents the contrast of the turbulent kinetic energy of van tail. Since the smoothness of air flow has been improved and air flow becomes more regular, the turbulent kinetic energy of van tail will be reduced. The figure shows that the low pressure area of the van model with drag reduction device in tail is significantly less than that of the original model. And drag vortex will be shorter. The concentration area of turbulent kinetic energy becomes smaller and the turbulent kinetic energy of the central region has also been reduced. The simulation results show that the aerodynamic drag coefficient of the van model with drag reduction device in tail is 0.6431, which is reduced by 5.773 % compared with the original model. The force measurement and pressure measurement experiments were carried out in the wind tunnel by the authors of the literature [5]. The research showed that the drag of the truck model with the pneumatic attachment of back fence was reduced by 7.19 %. This shows that the tail drag reduction device in this paper can reduce the drag coefficient of the truck.

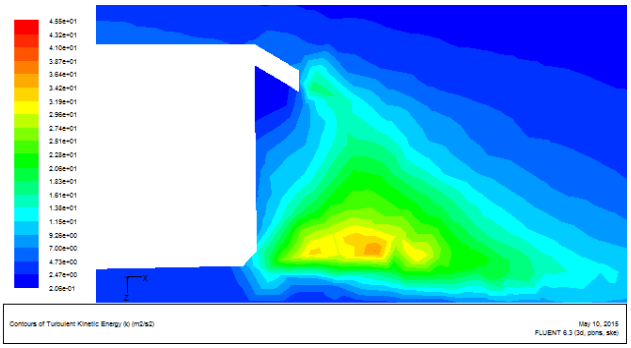

a) The van model with drag reduction device in tail

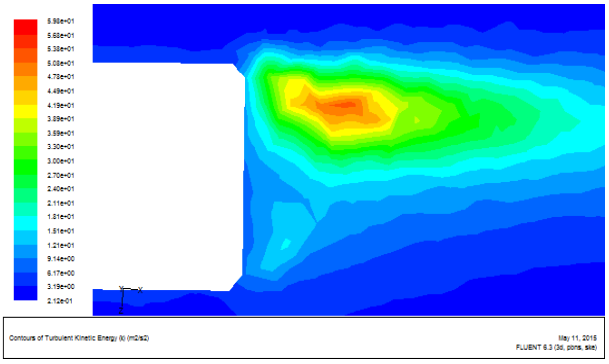

b) The original model

Figure 10. Contrast of the turbulent kinetic energy of the van tail (center section).

5.2 Design of drag reduction device at bottom and comparative analysis

In the area between the front and rear wheels of the van a very complex phenomenon of turbulence will be formed because of the long distance between its front and rear wheels. The complex turbulence will greatly increase air resistance, which affects the van speed and greatly increases fuel consumption. In order to improve the smoothness of the air flow at the bottom of the van, a kind of drag reduction structure at the bottom of the van is presented. The device, located between the front and rear wheels of van, is an air flow passage that is composed of side plates. The specific structure is shown in Fig. 11.

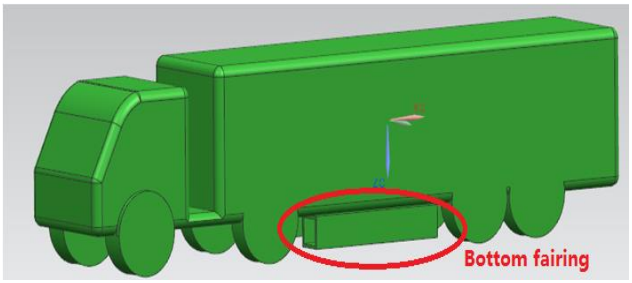

Figure 11. Van model with drag reduction device at the bottom.

Fig. 12 shows the contrast of the speed contour of van bottom. The figure shows that the bottom airflow velocity of the improved van is more uniform. Because the air flow at the bottom of the van is more complex, the turbulent kinetic energy is relatively large, which is a factor in producing van resistance. Fig. 13 shows the contrast of the turbulent kinetic energy of the van bottom. After installation of the bottom deflector, the smoothness of the airflow is significantly improved and the turbulent kinetic energy and aerodynamic drag are significantly reduced. The simulation results show that the aerodynamic drag coefficient of the van model with the drag reduction device at the bottom is 0.6238, which is reduced by 7.136 % compared with the original model. The flow field of trucks with 4 kinds of underbody skirt and no skirt were studied by the authors in the literature [6]. The aerodynamic drag coefficient of the prototype truck without underbody skirt is 0.556. And the aerodynamic drag coefficient of the truck with the underbody skirt is 0.546. The drag coefficient was decreased by 1.83 %. This shows that the bottom

drag reduction device in this paper can reduce the drag coefficient of the truck.

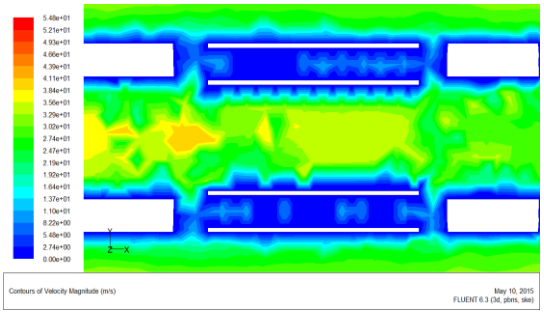

a) Van model with drag reduction device at the tail

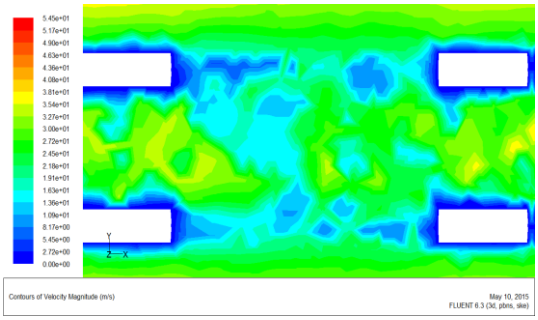

b) Original model

Figure 12. Contrast of the speed contour of van bottom.

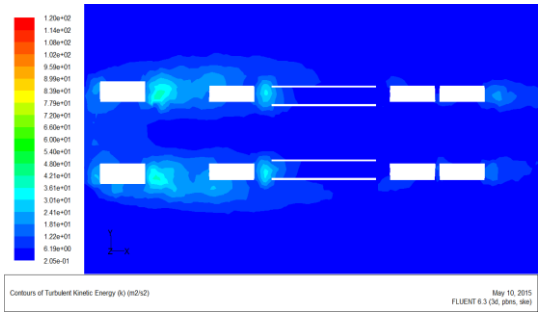

a) Van model with drag reduction device at the tail

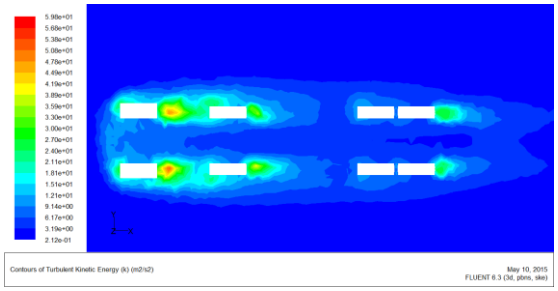

b) Original model

Figure 13. Contrast of turbulent kinetic energy at van bottom.

5.3 Design of drag reduction device in front and comparative analysis

A high degree of air flow separation and vortex are produced between the cab and the container. In order to reduce airflow resistance here and achieve a little smoother air flow, a drag reduction device is installed between the cab and the container, as shown in Fig. 14.

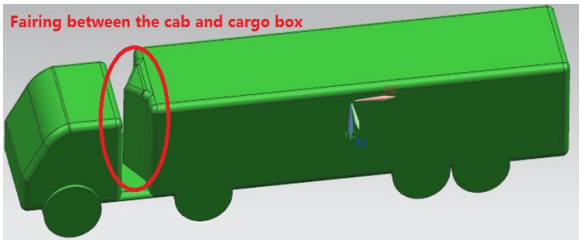

Figure 14. Van model with drag reduction device in front.

Fig. 15 shows the contrast of the pressure contour of the symmetry plane of the van, showing a smoother air flow between the container and cab of the improved van as well as reduced vortex. Pressure in the front of the improved van is reduced. Fig. 16 shows the contrast of the turbulent kinetic energy at the top of the van, which reveals that the turbulent kinetic energy of the van model with drag reduction device in front is reduced compared to the original model.

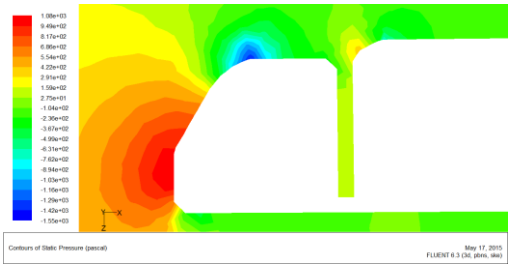

a) Van model with drag reduction device in front

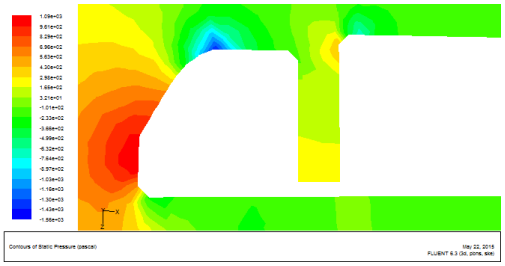

b) Original model

Figure 15.Contrast of the pressure contour of the symmetry plane of the van.

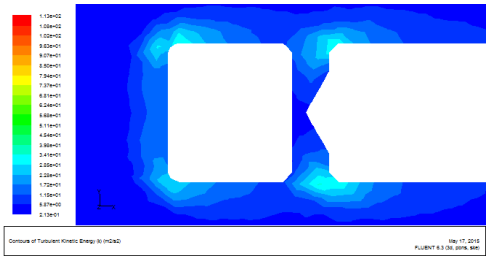

a) Van model with drag reduction device in front

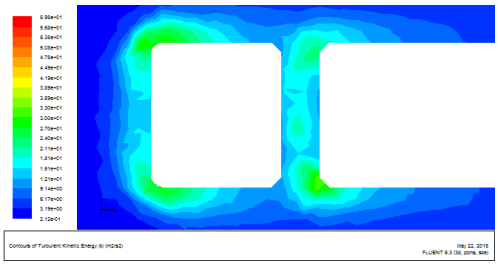

b) Original model

Figure 16. Contrast of the turbulent kinetic energy at the van top.

The simulation results show that the aerodynamic drag coefficient of the van model with drag reduction device in front is 0.6522, which is reduced by 4.44 % compared with the original model. According to the performance test of the same truck model conducted by the authors in the literature [3], the aerodynamic drag coefficient of the truck model was decreased by 10 % after the installation of the shroud. This shows that the front drag reduction device in this paper can reduce the drag coefficient of the truck. Table 2 shows the contrast of the air resistance coefficient between the van model with drag reduction device and the original model.

Table 2. Air resistance coefficient of different van models

Model	Air resistance coefficient	Percentage of optimization (%)
Original model	0.6825	
Van model with drag reduction device at the tail	0.6431	5.773
Van model with drag reduction device at the bottom	0.6238	7.136
Van model with drag reduction device in front	0.6522	4.440

5 Conclusions

1) The aerodynamic drag of the van is mainly concentrated at the top of the van cab and the van tail. The complex vortex is formed because the airflow at the top of the van cab is obstructed by the cargo compartment. At the van tail, the air flow from the top, the sides and the bottom of the van tail is collected and a vortex is formed.
2) Three kinds of van fairing are established based on an aerodynamic drag reduction mechanism. Three kinds of drag reduction structures are installed respectively at the rear, bottom and front of the van on the basis of the original van model. Three kinds of van fairing have a great influence on the aerodynamic characteristics of the van.
3) The aerodynamic drag coefficient of the original van model is the largest. Three kinds of additional drag reduction structures of the van have a great effect of drag reduction. The largest decline of the aerodynamic drag coefficient of the van is 7.136 %. Three kinds of additional drag reduction devices can reduce the turbulent vortices generated in the outflow field of the van to a certain extent so that the aerodynamic drag is minimized.

Acknowledgements

This paper is supported by education and research programs for middle aged and young scholars of Fujian province of China (grant No. JA15367).

References

[1] Wang, P., Gu, Z. et al.: *Numerical simulation and improvement of the aerodynamic characteristics of semi-trailer container truck*, Automotive engineering, 32 (2010), 5, 387-393.
[2] Gong, Xu., Gu, Z. et al.: *Shape optimization of wind deflector in container semitrailer based on approximate model*, Automotive engineering, 33 (2011), 1, 38-42.
[3] Wang, J., Hu, X. J. et al.: *Numerical simulation of influence of guide cowl on light-duty van aerodynamic characteristics*, Journal of Jilin University (Engineering and technology edition), 38 (2008), 1, 12-16.

[4] Song, X., Hu, S., Zhang, W.: *Numerical simulation for the exterior flow field around a round-roof van and optimization design of its aerodynamic attachment*, Automotive engineering, 29 (2007), 9, 797-811.
[5] Zhang, P. F., Wang, J. J., Tang, Q.: *Experimental investigation on the aft-body drag reduction of the tractor-trailer truck by aerodynamic add-on device*, Journal of experiments in fluid mechanics, 23 (2009), 3, 12-15, 2009.
[6] Hu, X., Yang, B. et al. : *Aerodynamic drag reduction of van based on underbody skirt*, Journal of Jilin University (Engineering and technology edition), 41(2011), 2, 108-113.
[7] Yang, X. L., Hu, K. Y.: *Study of a Passive Drag Reduction Technology for Trucks*, Journal of Hunan University (Natural Sciences), 39 (2012), 3, 33-37.
[8] Wang, D. et al: *Numerical simulation of a 3-D flow field around a Van-body truck*, Transactions of the chinese society of agricultural machinery, 35 (2004), 3, 20-23.
[9] Liu, C., Wang, J. Y. et al.*: Effect of gap between driver cab and freight body of heavy-duty truck on its aerodynamic characteristic*, Journal of Jilin University (Engineering and technology edition), 37 (2007), 2, 280-285.
[10] Guo, P., Hu, X. J., Zhu, Y. Y. et al.: *Investigation on aerodynamic drag reduction of commercial truck based on external styling of cab*, Applied Mechanics and Materials, 307 (2013), 186-191.
[11] Chowdhury, H., Moria, H., Ali, A. et al.: *A study on aerodynamic drag of a semi-trailer truck*, Procedia Engineering, 56 (2013), 201-205.
[12] Choi, H., Lee, J., Park, H.: *Aerodynamics of heavy vehicles*, Annual Review of Fluid Mechanics, 46 (2014), 441-468.
[13] Yang, H. B., Hu, X. J., Li, T. F.: *Numerical analyses to investigate the impact of external sun visor on aerodynamic drag of heavy-duty commercial truck*, Applied mechanics and materials, 602 (2014), 787-790.
[14] Choi, H, Lee, J, Park, H.: *Aerodynamics of heavy vehicles*, Annual Review of Fluid Mechanics, 46 (2014), 441-468.
[15] Taherkhani, A. R., de Boer, G. N., Gaskell, P. H. et al.: *Aerodynamic drag reduction of emergency response vehicles*, Advances in Automobile Engineering, 4 (2015), 2, 2-6.
[16] Salati, L., Cheli, F., Schito, P.: *Heavy truck drag reduction obtained from devices installed on the trailer*, SAE international journal of commercial vehicles, 8(2015), 747-760.
[17] Khalighi, B., Balkanyi, S. R., Bernal, L. P.: *Experimental investigation of aerodynamic flow over a bluff body in ground proximity with drag reduction devices*, International Journal of Aerodynamics, 3(2013), 4, 217-233.
[18] Liu, Y., Tang, A. P., Liu, K. T., et al.: *Numerical simulation on the aerodynamic force of the iced conductor for different angles of attack*. Engineering Review, 35 (2015), 2, 157-169.
[19] Čarija, Z., Marušić, E., Novak, Z., et al.: *Numerical analysis of aerodynamic characteristics of a bumped leading edge turbine blade*, Engineering Review, 34 (2014), 2, 93-101.
[20] Bian, M., Wang, Z., Gao, H.: *Analysis for muffler of 1P68F small gasoline engine, Small internal combustion engine and motorcycle*, 38 (2009), 68-69.